Artificial Organs
32(5):388–397, Blackwell Publishing, Inc.

Nanobioengineered Electrospun Composite Nanofibers and Osteoblasts for Bone Regeneration

*Jayarama Reddy Venugopal, †Sharon Low, †‡Aw Tar Choon, *A. Bharath Kumar, and *Seeram Ramakrishna

**Nanoscience and Nanotechnology Initiative, Division of Bioengineering, National University of Singapore, Singapore; †StemLife Sdn BhD, Kuala Lumpur, Malaysia; ‡Department of Laboratory Medicine, Changi General Hospital, Singapore, and School of Medicine and Health Sciences, Monash University, Malaysia*

Abstract: Bone defects represent a medical and socioeconomic challenge. Engineering bioartificial bone tissues may help to solve problems related to donor site morbidity and size limitations. Nanofibrous scaffolds were electrospun into a blend of synthetic biodegradable polycaprolactone (PCL) with hydroxyapatite (HA) and natural polymer gelatin (Gel) at a ratio of 1:1:2 (PCL/HA/Gel) compared to PCL (9%), PCL/HA (1:1), and PCL/Gel (1:2) nanofibers. These fiber diameters were around 411 ± 158 to 856 ± 157 nm, and the pore size and porosity around 5–35 μm and 76–93%, respectively. The interconnecting porous structure of the nanofibrous scaffolds provides large surface area for cell attachment and sufficient space for nutrient transportation. The tensile property of composite nanofibrous scaffold (PCL/HA/Gel) was highly flexible and allows penetrating osteoblasts inside the scaffolds for bone tissue regeneration. Fourier transform infrared analysis showed that the composite nanofiber contains an amino group, a phosphate group, and carboxyl groups for inducing proliferation and mineralization of osteoblasts for in vitro bone formation. The cell proliferation (88%), alkaline phosphatase activity (77%), and mineralization (66%) of osteoblasts were significantly ($P < 0.001$) increased in composite nanofibrous scaffold compared to PCL nanofibrous scaffolds. Field emission scanning electron microscopic images showed that the composite nanofibers supported the proliferation and mineralization of osteoblast cells. These results show that the fabrication of electrospun PCL/HA/Gel composite nanofibrous scaffolds has potential for the proliferation and mineralization of osteoblasts for bone regeneration. **Key Words:** Electrospinning—Polycaprolactone—Hydroxyapatite—Gelatin—Composite nanofibers—Osteoblast—Mineralization—Regeneration.

In recent years, nanoscale sciences and engineering have provided new avenues for engineering biocomposite materials with macromolecular size and even down to molecular-scale precision. The resultant biocomposite materials have been demonstrated to have enhanced properties and applicability, and these materials are expected to enable technologies for successful development in the applications of nanomedicine. The goal of tissue engineering is to "restore function through the delivery of living elements which become integrated into patient" (1). Repair of large bone defects is still a challenge for orthopedic, reconstructive, and maxillofacial surgeons (2). Every year, millions of people suffer from bone defects arising from trauma, tumor, or bone diseases, and of course many people die due to insufficient ideal bone substitute. There is a long history of using autogeneic and allogeneic bones in the treatment of bone defects. Even though autogeneic bone performs better functions in terms of biocompatibility and other factors, it needs secondary surgery to procure donor bone from the patient's own body. Allogeneic bone bears risk of infections and immune responses, which may even cause other health problems, thus affecting the quality of life. As an alternative, synthetic biomaterials have been developed for the repair of bone, and were clinically tested (3).

doi:10.1111/j.1525-1594.2008.00557.x

Received February 2007; revised July 2007.
Address correspondence and reprint requests to Dr. Jayarama Venugopal, Nanoscience and Nanotechnology Initiative, Division of Bioengineering, National University of Singapore, Block E3, #05-12 NUSNNI, 9 Engineering Drive 1, Singapore 117576. E-mail: engjrv@nus.edu.sg

A number of novel approaches have been developed for the fabrication of biomaterial-based three-dimensional scaffolds (4). The electrospinning method has been actively explored recently; because of its simple process, it offers ultrafine polymer fibers, high specific surface area, and the possibility of various modifications (5,6). The features of nanofiber mats are morphologically similar to extracellular matrix (ECM) of the natural tissue, which are characterized by a wide range of pore diameter distribution, high porosity, effective mechanical properties, and specific biochemical properties (7,8). The large surface-area-to-volume ratio of nanofibers combined with their porous structures favors cell adhesion, proliferation (9), migration (10), and differentiation (11); these are the desired properties for engineering tissues (12). Pore interconnectivity positively influences bone deposition rate and depth of infiltration in vitro (13) and in vivo (14). Regular interconnected pores provide spacing for the vasculature required to nourish new bone and to remove waste products (15). Studies suggest that microporosity (pores < 20 μm) improves bone growth into scaffolds by increasing surface area for protein adsorption, increasing ionic solubility in the microenvironment (16), and providing attachment points for osteoblasts (13,17).

Conversely, many researchers have investigated polymer composites with inorganic materials used as scaffolds for tissue engineering (18). Hydroxyapatite (HA) is a ceramic with chemical composition similar to the mineral component of bone that possesses good properties of ideal hardness, biocompatibility, osteoconductivity, a certain degree of bioactivity, and high resistance to moisture, and has been used in a variety of oral and maxillofacial applications (17,19). Some research groups have tried to develop synthetic bone, which was prepared by the coprecipitation reaction of HA nanocrystals in soluble collagen (Col). These efforts have met with partial success in the preparation of HA–Col nanocomposite, which is similar to the nanostrucuture of real bone. Col is easily degraded and resorbed by the body, and allows good attachment to cells. However, its mechanical properties are relatively low ($E \sim 100$ MPa) in comparison to bone ($E \sim 2$–5 GPa) (20), and it is therefore highly cross-linked or found in composites, such as Col–glycosaminoglycans for skin regeneration or Col/HA for bone remodeling (21). The main practical problems with Col are its cost and poor definition of commercial sources of this material, which makes it difficult to follow up on well-controlled processing. Therefore, in the present study, Col was replaced by gelatin (Gel), a protein produced by the partial hydrolysis of Col extracted from skin, bone, cartilage, ligaments, etc. Mixing Gel with other synthetic polymers, sometimes called bioartificial polymeric materials, has frequently been adopted by other researchers. This approach is feasible to reduce the potential problem of cytotoxin, as a result of using a chemical cross-linking reagent, but also provides a compromise solution for overcoming the shortcomings of synthetic and natural polymers, that is, producing a new biomaterial with excellent biocompatibility and improved mechanical and physical/chemical properties. In the present study, polycaprolactone (PCL) was blended with HA and Gel, and electrospun into composite nanofibers to provide proper balance between biocompatibility, biodegradability, osteoconductivity, and mechanical stability for engineering bone tissue regeneration.

MATERIALS AND METHODS

Materials

Human fetal osteoblast (hFOB) cells were obtained from American Type Culture Collection (Arlington, VA, USA). Dulbecco's Modified Eagle's Medium (DMEM)/Nutrient Mixture F-12 (HAM), fetal bovine serum (FBS), antibiotics, and trypsin–ethylenediaminetetraacetic acid (EDTA) were purchased from GIBCO Invitrogen, Carlsbad, CA, USA. PCL (MW 80 000) was from Aldrich Chemical Company, Milwaukee, WI, USA. CellTiter 96 AQ_{ueous} one solution was purchased from Promega, Madison, WI, USA. Gelatin Type-A (porcine) and cetylpyridinium chloride were purchased from Sigma, St. Louis, MO, USA. Crystalline HA (30.25 ± 4.43 nm) was generously provided by the Department of Metallurgical and Materials Engineering, Indian Institute of Technology, Chennai, India.

Fabrication and characterization of PCL/HA/Gel composite nanofibers

PCL (9% w/w) and PCL/HA (PCL 7%/HA 7%) were dissolved in methanol/chloroform (1:3) under stirring conditions for 2 days. The ratio of PCL/HA/Gel was 1:1:2 (PCL 2%/HA 2%/Gel 4%) and PCL/Gel (PCL 3%/Gel 6%) w/w dissolved in 2,2,2-trifluoroethanol. These samples were fabricated by an electrospinning process, 1.5 mL/h employing an applied voltage of 11 kV using a high-voltage power supply (Gamma High Voltage Research, Ormond Beach, FL, USA). The PCL/HA/Gel solution was delivered 1 mL/h through a syringe pump (KD-100, KD Scientific, Inc., Holliston, MA, USA) for controlling the mass flow rate of electrospinning and applied voltage of 13 kV using a high-voltage power supply.

The ground collection plate of aluminum foil was located around 12 cm from the needle tip. A positively charged jet was formed from the syringe needle, and nanofibers were sprayed onto the grounded aluminum foil target (5). The ambient condition of the spinning apparatus was controlled to be 23°C and 60% humidity. Coverslips of different sizes were spread onto the aluminum foil target to collect the nanofibers to investigate biocompatibility by culturing cells as well as to observe the structure and properties of nanofibers.

Nanofibers collected on the aluminum foil were used for the characterization and assessment of tensile strength. These nanofibers were dried under vacuum at room temperature overnight. Electrospun nanofibers were sputter coated with gold (JEOL JFC-1600, Auto Fine Coater, Tokyo, Japan) and visualized by field emission scanning electron microscopy (FESEM) (FEI–QUANTA 200F, Eindhoven, The Netherlands) at an accelerating voltage of 10 kV for characterization. The fiber diameter was measured with FESEM images using Image J software (National Institutes of Health, Bethesda, MD, USA). Chemical analysis of PCL/HA/Gel nanofibrous scaffolds was analyzed by Fourier transform infrared (FT-IR) spectroscopy (Avatar 380, Thermo Nicolet, Waltham, MA, USA) over a range between 4000 and 400 cm^{-1} at 2 cm^{-1} resolution averaging 100 scans. The pore size was measured by bubble point pressure (22), and the porosity was estimated by weight and volume of the sample (23).

Mechanical characterization of nanofibrous scaffolds

Tensile properties of electrospun nanofibrous scaffolds were determined with a tabletop MicroTester (Instron 5845, Norwood, MA, USA) using low-force load cell of 10 N capacity. Strip-shaped specimens (30×6 mm^2) were tested at a crosshead speed of 10 mm/min. The ambient condition was controlled to be 25°C and 74% humidity. At least six samples were tested for each type of electrospun nanofibrous scaffold. Ultimate strength, Young's modulus, as well as tensile elongation were calculated based on the generated tensile stress–strain curves (10,17).

Wettability of nanofibrous scaffolds

The water contact angles of PCL, PCL/HA, PCL/Gel, and PCL/HA/Gel nanofibrous scaffolds were measured using a contact angle measurement system (VCA Optima XE Video Contact Angle System, Crest Technology Pte Ltd., Singapore) mounted with a CCD camera at ambient temperature. The nanofibrous scaffolds were carefully placed on a sample stage, and a single drop of distilled water was applied to the mesh surface to measure the angle, and averaged.

hFOB cell culture

hFOB cells were cultured in DMEM/F12 medium (1:1) containing 10% FBS in 75 cm^2 cell culture flasks. The osteoblast culture was maintained at 37°C in a humidified CO_2 incubator for 6 days and fed every 3 days, and hFOBs were harvested from the third passage cultures by trypsin–EDTA treatment, and replated. Populations of cell lines used in this experiment were between passages 5 and 6.

Processing of hFOB cells for FESEM

Nanofiber scaffolds were collected in 15 mm cover glasses (0.02–0.03 mm thickness of the nanofiber scaffold in cover glass) and sterilized under UV light for 3 h. These scaffolds were again sterilized with 70% ethanol (30 min), then washed with phosphate-buffered saline (PBS) (15 min) three times and finally soaked in complete medium overnight. hFOBs were seeded (2×10^4 cells/cm^2) on PCL, PCL/HA, PCL/Gel, PCL/HA/Gel nanofibrous scaffolds, and tissue culture plate (TCP—control) on 24-well plates. After 6 days of experiment, hFOBs grown on scaffolds were washed with PBS to remove nonadherent cells, and then fixed in 3% glutaraldehyde for 3 h at room temperature, dehydrated through a series of graded alcohol solutions, and finally dried into hexamethyldisilazan overnight. Dried cellular constructs were sputter coated with gold and observed under FESEM at an accelerating voltage of 10 kV.

3-(4,5-Dimethylthiazol-2-yl)-5-(3-carboxymethoxyphenyl)-2-(4-sulfophenyl)-2H-tetrazolium, inner salt (MTS) assay for hFOB cell proliferation

hFOB cells were seeded (2×10^4 cells/cm^2) on sterilized PCL, PCL/HA, PCL/Gel, PCL/HA/Gel nanofibrous scaffolds, and TCP on 24-well plates. Cell proliferation was monitored after 2, 4, and 6 days by MTS assay. In order to monitor cell adhesion and proliferation on different substrates, the number of cells was determined by using colorimetric MTS assay (CellTiter 96 AQ_{ueous} assay). The mechanism behind this assay is that metabolically active cells react with tetrazolium salt in MTS reagent to produce a soluble formazan dye that can be observed at 490 nm. The cellular constructs were rinsed with PBS followed by incubation with 20% MTS reagent

in serum-free medium for 3 h. Thereafter, aliquots were pipetted into 96-well plates, and the samples were read in a spectrophotometric plate reader at 490 nm (FLUOstar OPTIMA, BMG Labtech, Offenburg, Germany).

Alkaline phosphatase (ALP) activity

ALP is used to measure ALP activity by a kinetic rate method using 2-amino-2-methyl-1-propanol buffer. In this reaction, ALP catalyzes the hydrolysis of colorless organic phosphate ester substrate, *p*-nitrophenylphosphate, to a yellow product, *p*-nitrophenol, and phosphate. This reaction occurs at an alkaline pH of 10.3. Nanofibrous scaffolds with hFOBs were washed twice with PBS and added with 1 mL of 10 mM Tris buffer to isolate the sample. The sample (1 mL) was again sonicated for 2 min at 4°C. The sonicated sample was centrifuged at 3000 rpm for 5 min at 4°C, then the supernatant was used for the assay of ALP activity. The SYNCHRON LX system (Beckman Coulter, Fullerton, CA, USA) automatically proportions the appropriate sample and reagent volumes into the cuvette. The ratio used is one part of sample to 50 parts reagent. The system monitors the change in absorbance that is directly proportional to the activity of ALP in the sample and is used by SYNCHRON LX system to calculate and express the ALP activity.

Mineralization of hFOB

Alizarin red-S (ARS) is a dye that binds selectively calcium salts and is widely used for calcium mineral histochemistry. ARS staining was used to detect and quantify mineralization (24). Nanofibrous scaffolds with hFOB cells (construct) were washed three times in PBS and fixed in ice-cold 70% ethanol for 1 h. These constructs were washed three times with dH_2O and stained with ARS (40 mM) for 20 min at room temperature. After several washes with dH_2O, these constructs were observed under optical microscope, and the stain was desorbed with the use of 10% cetylpyridinium chloride for 1 h. The dye was collected and the absorbance was read at 540 nm in spectrophotometer (Thermo Spectronics, Waltham, MA, USA).

Statistical analysis

All quantitative results were obtained from triplicate samples. Data were expressed as the mean ± standard deviation. Statistical analysis was carried out using the unpaired Student's *t*-test and one-way analysis of variance. A value of $P < 0.05$ was considered to be statistically significant.

RESULTS AND DISCUSSION

Characterization of composite nanofibers

The success rate of tissue engineering approaches was highly dependent on the properties of scaffold used as a cell carrier. Generally, scaffold design was based on degradability, biocompatibility, high surface area/volume ratio, osteoconductivity, and suitable mechanical properties for engineering tissues (25). A crucial point for a scaffold to be successful, especially in bone tissue engineering, is the combination of structural/mechanical properties of polymer structure and biological activities, all of them playing a critical role in cell seeding, proliferation, and new tissue formation. Bone substitutes allow repair mechanism by providing a permanent or temporary porous device (scaffold) that reduces the size of the defect. The interest in temporary substitutes is that they permit a mechanical support until the tissue has regenerated and remodeled itself naturally. As electrospun pure Gel fibrous scaffold can dissolve and disappear at normal cell culture temperature at 37°C (10), the PCL/Gel and PCL/HA/Gel nanofibrous scaffolds cannot dissolve in normal temperature, but they are used to investigate the influence of Gel on cell performance and HA for the mineralization of osteoblasts. When placed in cell culture medium, PCL/HA/Gel nanofibrous scaffolds, unlike other scaffolds made of natural polymers did not disintegrate, even in the absence of cross-linking.

The electrospun nanofiber morphologies of PCL, PCL/HA, PCL/Gel, and PCL/HA/Gel were observed by FESEM (Fig. 1), and diameters are formed in the range of 411 ± 158 to 856 ± 157 nm, and the pore size and porosity were around 5–35 μm and 76–93%, respectively (Table 1). The fibrous architecture mimicked the ECM and assisted in maintaining a normal phenotype of the cells. This composite nanofiber surface topography plays a crucial role in regulating initial cell behaviors, such as cell adhesion, which can also influence cellular viability and proliferation in later stage of cells (26). Water contact angle measurement shows that the nanofibrous scaffold surface morphologies were either hydrophobic or hydrophilic suitable for cell adhesion process to vastly different extents (Table 1). The mechanical properties of the scaffolds were assessed using compressive and tensile mechanical tests. The average tensile modulus of all nanofibers was around 3.9–28.7 MPa, and tensile strain was 82–142% (Table 2). The data represent tensile strain of PCL/HA/Gel showing sufficient mechanical properties to support proliferation and mineralization of osteoblast cells.

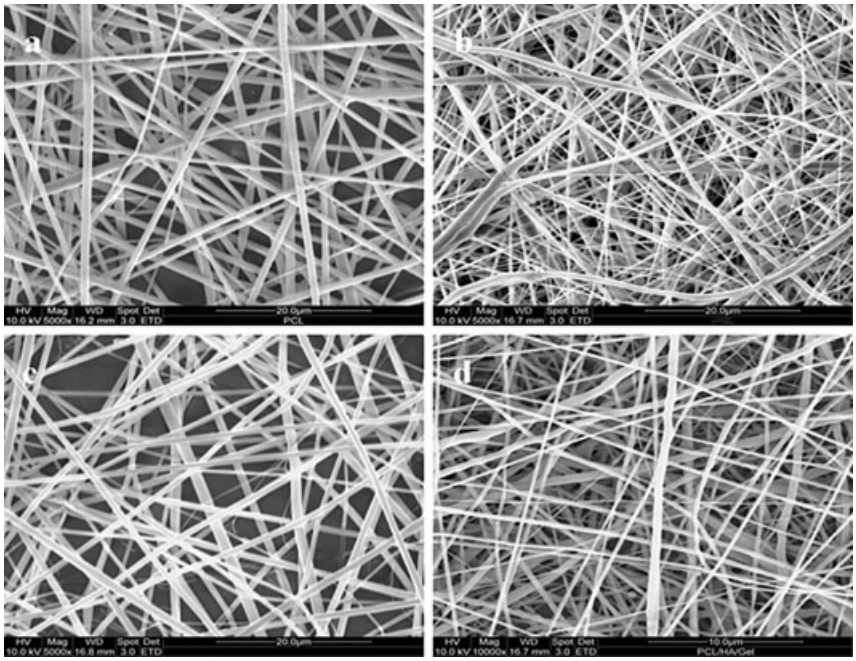

FIG. 1. FESEM images of electrospun (a) PCL (9% w/w), (b) PCL/HA (1:1), (c) PCL/Gel (1:3), and (d) PCL/HA/Gel (1:1:2) nanofibers.

FT-IR analysis of PCL/HA/Gel composite nanofibrous scaffold showed typical bands such as N—H stretching at 3310 cm^{-1} for amide-A, C—H stretching at 3068 cm^{-1} for amide-B, C═O stretching at 1600–1700 cm^{-1} for amide I, N—H deformation at 1500–1550 cm^{-1} for amide II, and N—H deformation at 1200–1300 cm^{-1} for amide III band in PCL/Gel and PCL/HA/Gel nanofibrous scaffolds were found (Fig. 2c,d). PCL/HA/Gel nanofibers showed that nearly identical spectra, with a P—O stretch vibration absorbance peak at around 1040 cm^{-1} and P—O bend vibration absorbance peaks at around 604 and 566 cm^{-1}, as well as carbonate C—O bend vibration absorbance peak at about 874 cm^{-1} and C—O stretch vibration absorbance from 1400 to 1480 cm^{-1} (Fig. 2c,d) in each spectrum (27). Calcium (Ca_2^+) and phosphate ions (PO_4^-) exist at the HA nanocrystal surface. If self-organization had occurred from electrostatic interactions between such ions and functional groups (e.g., Ca_2^+ vs. COO^- or PO_4^- vs. NH_3), their influence should be detectable with infrared spectroscopy.

PCL/HA/Gel nanocomposite samples have nonstoichiometric apatite compositions, because the resonance frequencies are close to 1020 cm^{-1}, identified as PO_4^- band in nonstoichiometric apatite (Fig. 2b,d). We can observe CO_3^- band at 980 cm^{-1}, indicating the incorporation of CO_3^- into both OH^- and PO_4^- in apatite lattice (Fig. 2b–d). The phosphate band between 1000 and 1150 cm^{-1} indicates that the

TABLE 1. *Characterization of electrospun nanofiber membranes*

	PCL	PCL/HA	PCL/Gel	PCL/HA/Gel
Contact angle (degrees)	125.84	128.94	0	0
Average fiber diameter (nm)	632 ± 147	807 ± 161	856 ± 157	411 ± 158
Pore size (μm)	5–20	6–22	6–32	7–35
Porosity (%)	76	92	89	93

TABLE 2. *Tensile properties of electrospun nanofiber membranes*

Nanofibrous membrane	Tensile strength (MPa)	Elastic modulus (MPa)	Elongation at break (mm/mm)	Tensile strain (%)
PCL	2.70	4.96	1.26	104
PCL/HA	1.25	3.9	0.85	82
PCL/Gel	1.27	28.7	1.37	136
PCL/HA/Gel	1.2	7.4	1.43	142

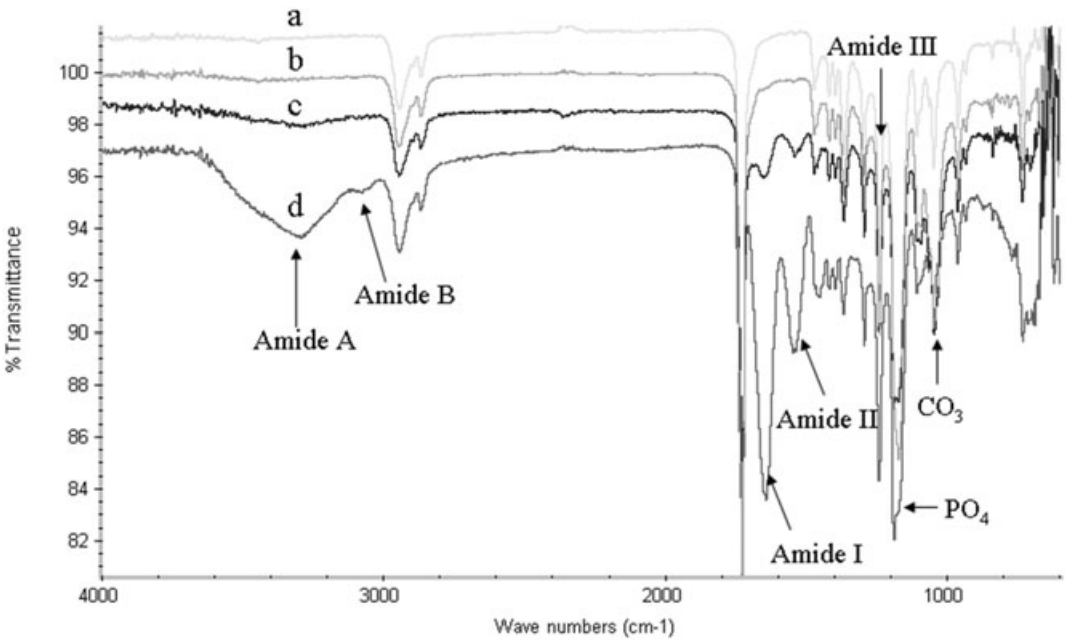

FIG. 2. FT-IR spectroscopic analysis of (a) PCL, (b) PCL/HA, (c) PCL/Gel, and (d) PCL/HA/Gel nanofibers.

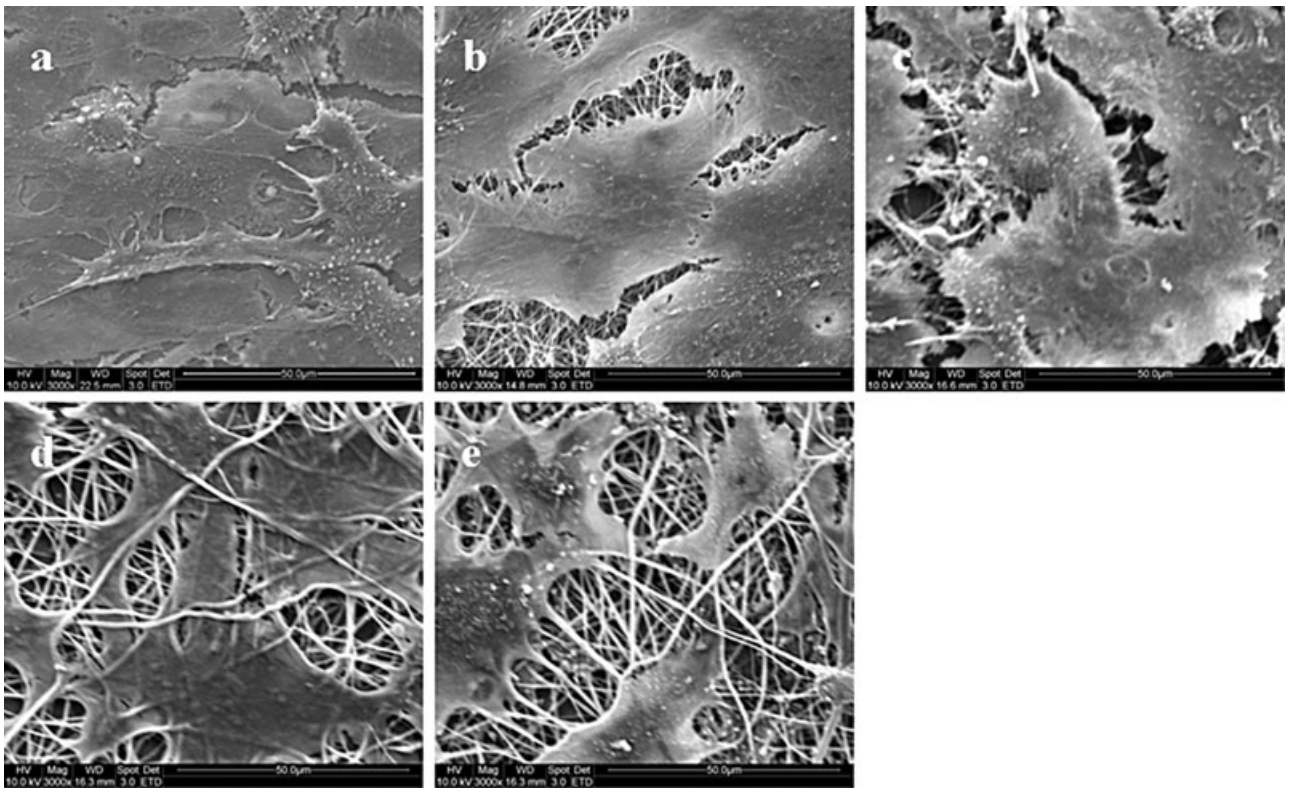

FIG. 3. FESEM micrographs showing migration of hFOB inside the nanofibrous scaffold after 4 days of culture in (d) and (e). (a) TCP/osteoblasts, (b) PCL/osteoblasts, (c) PCL/HA/osteoblasts, (d) PCL/Gel/osteoblasts, and (e) PCL/HA/Gel/osteoblasts.

organic–inorganic interaction between HA crystals and Gel macromolecules had induced a nonstoichiometric apatite composition (4). This composite nanofiber contains an amino group, a phosphate group, and carboxyl groups for inducing proliferation and mineralization of osteoblasts for bone regeneration.

Composite nanofibrous scaffold and osteoblasts for mineralization

The composite nanofibers showed improved biological properties in terms of human osteoblast cell response compared to PCL nanofibers. Figure 3d,e showed cellular ingrowth after 4 days of osteoblasts cultured on biocomposite nanofibrous scaffolds. While loosely interlaced fibrous structure and the weak nanoscale fibers can provide the least obstruction and matched mechanical properties for cell movements, it seems that the presence of appropriate molecular signals on nanofiber surface can also guide or attract the living cells to enter into the matrix through their amoeboid movement. The FESEM micrographs of osteoblasts cultured on PCL/HA/Gel composite nanofibrous scaffolds for 6 days showed that the cells spread actively on fibrous mesh and penetrate inside the scaffolds (Fig. 4d,e) instead of just attaching on the surfaces exhibited on the PCL nanofibrous scaffolds (Fig. 4b). The cell proliferation was quantified by MTS assay showing significantly ($P < 0.001$) higher cell proliferation (day 6) in PCL/HA/Gel composite nanofibers compared to PCL, PCL/HA, and PCL/Gel nanofibrous scaffolds (Fig. 5). The proliferation was significantly increased up to 88% compared to PCL nanofibers. Blending of Gel with PCL provides good hydrophilicity and cellular affinity with consistent release of Gel protein molecule from PCL/HA/Gel composite nanofibrous scaffolds, and HA initiating the mineralization of osteoblast cells. The cell adhesion and proliferation were also increased due to fiber size as well as variation in chemistry and properties of the nanofibrous scaffolds by the addition of Gel and HA. Zhang et al. studied Gel/PCL nanofibrous scaffolds; the Gel can be continuously released (leached out) over a time scale of more than 2 weeks in PBS solution at 37°C. The leaching kinetics can be governed by a progressive dissolution and diffuse mass transfer similar to that of an erosion process. These biocomposite porous nanofibers gradually leached out of the water-soluble Gel from Gel/PCL fibers (28). Moreover, the nanoscale HA crystals can improve the initial attach-

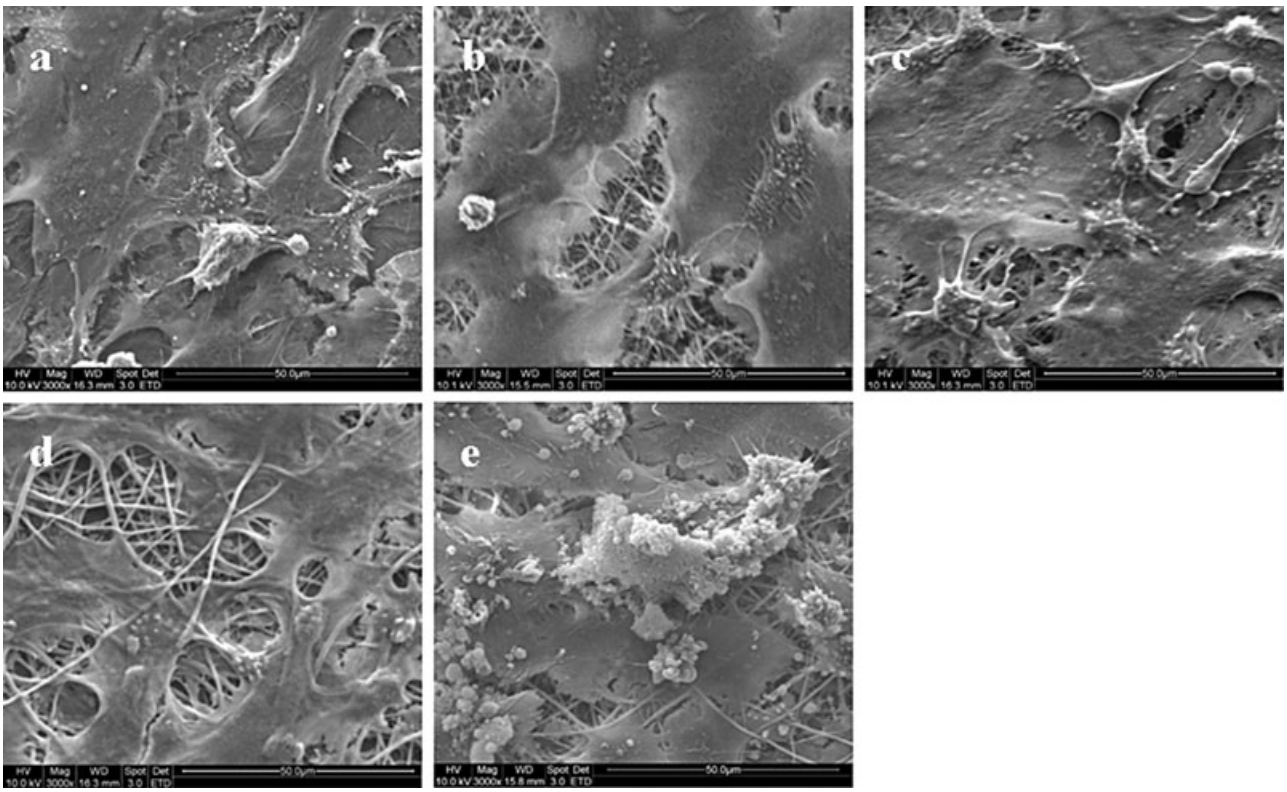

FIG. 4. FESEM micrographs of hFOB interaction with nanofibrous scaffold after 6 days of culture. (a) TCP/osteoblasts, (b) PCL/osteoblasts, (c) PCL/HA/osteoblasts, (d) PCL/Gel/osteoblasts, and (e) PCL/HA/Gel/osteoblasts.

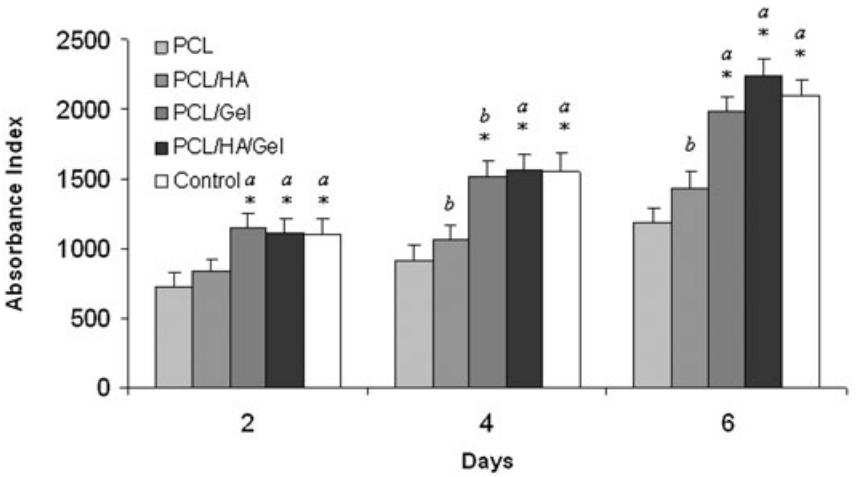

FIG. 5. The hFOB proliferation on PCL, PCL/HA, PCL/Gel, PCL/HA/Gel nanofibrous scaffolds, and control ($n = 6$). Bar represents means ± standard deviation. Asterisks (*t*-test, and *a* and *b* represent one-way analysis of variance) indicate significant difference in the measurement when compared to PCL nanofibrous scaffold (*$P < 0.001$; *a*, $P < 0.001$; *b*, $P < 0.05$).

ment of cells (29,30). The initial cell attachment was primarily affected by the binding of adhesion molecules and their subsequent mediation between cells and material surface; increased cell adhesion on nanocomposites might also be related to the involvement of adhesion proteins, such as fibronectin and vitronectin existing abundantly in serum (31,32). In tissue engineering, any degradable scaffold is meant to serve as a provisional matrix, that is, promoting cell adhesion, migration, and proliferation until the cell secretes and deposits its own ECM. In this context, our PCL/HA/Gel composite nanofibrous scaffold contains Gel, rather than Col for bone tissue formation (33).

The bone-forming potential of osteoblast cells was further analyzed by their expression of ALP activity, because ALP is an important phenotype for bone-forming cells (33). The present results noted that the ALP activity of cells at day 10 was significantly ($P < 0.001$) increased up to 77% in PCL/HA/Gel nanocomposites than PCL nanofibers (Fig. 6), confirming the crucial role of HA bio-ceramic component in the stimulation of bone cell response, and thus, its significance in bone regeneration. Furthermore, ALP appears to have a crucial role in the initiation of matrix mineralization, and expression of this enzyme is own-regulated after mineralization starts (34,35). Calcification occurs at nucleation sites known as matrix vesicles present in the lacunae of mineralizing cartilage. They are believed to accumulate Ca^{2+} and inorganic phosphate, which serves as a nucleating agent for the formation of HA, the main inorganic component of the bone. Figure 7 showed that the mineralization of osteoblasts significantly ($P < 0.001$) increased

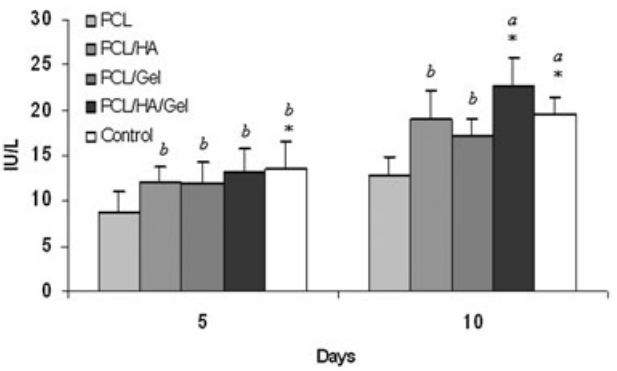

FIG. 6. ALP activity of osteoblasts culturing on PCL, PCL/HA, PCL/Gel, PCL/HA/Gel nanofibrous scaffolds, and control ($n = 6$). Bar represents means ± standard deviation. Asterisks (*t*-test, and *a* and *b* represent one-way analysis of variance) indicate significant difference in the measurement when compared to PCL nanofibrous scaffold (*$P < 0.001$; *a*, $P < 0.001$; *b*, $P < 0.05$).

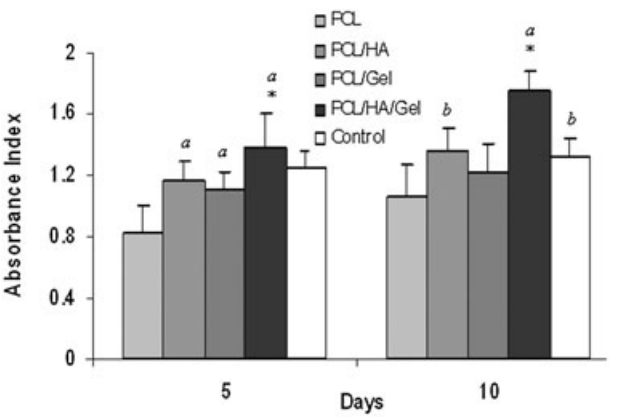

FIG. 7. ARS staining of mineral deposition in hFOB in (a) PCL, (b) PCL/HA, (c) PCL/Gel, (d) PCL/HA/Gel nanofibrous scaffolds, and control ($n = 6$). Bar represents means ± standard deviation. Asterisks (*t*-test, and *a* and *b* represent one-way analysis of variance) indicate significant difference in the measurement when compared to PCL nanofibrous scaffold (*$P < 0.001$; *a*, $P < 0.001$; *b*, $P < 0.05$).

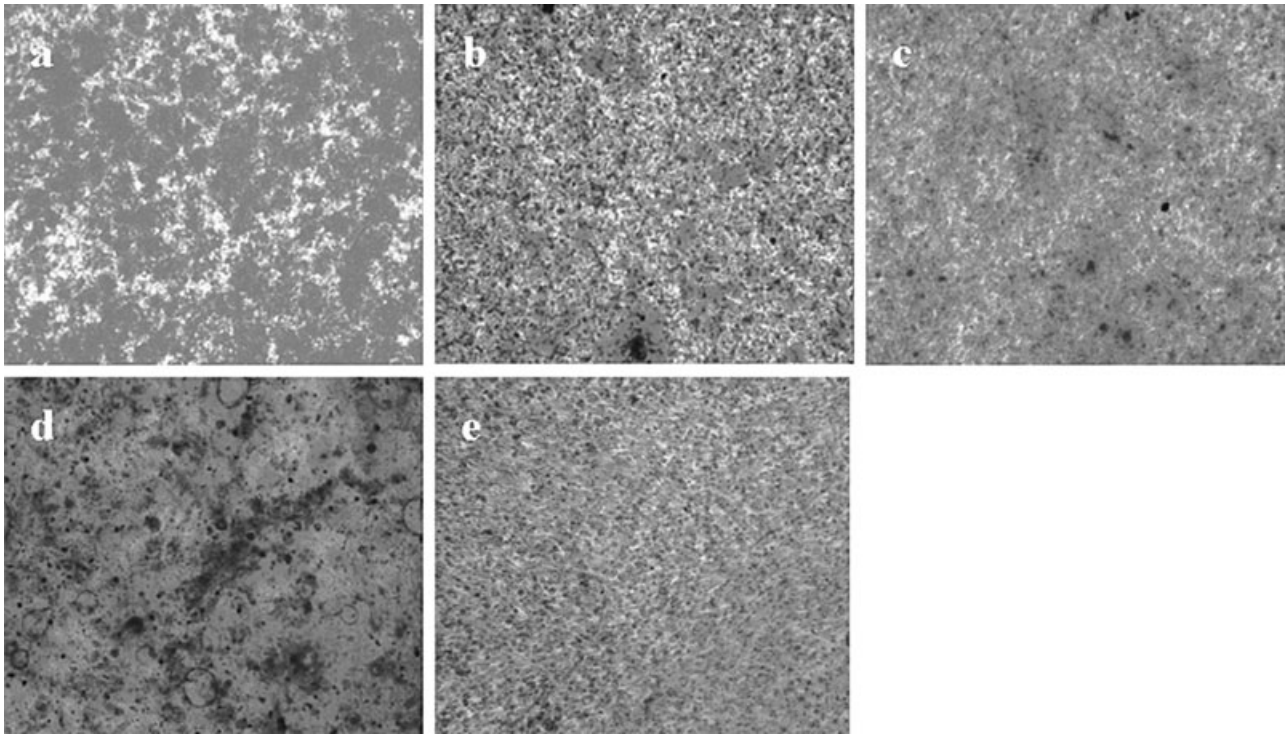

FIG. 8. ARS staining for calcium mineralization in hFOB on (a) PCL, (b) PCL/HA, (c) PCL/Gel, (d) PCL/HA/Gel nanofibrous scaffolds, and (e) TCP after 10 days of osteoblast cell culture.

in composite nanofibrous scaffold (PCL/HA/Gel) compared to the other three nanofibrous scaffolds, and the mineral particles are stained with ARS dye (Fig. 8). The mineral deposition by cultured osteoblasts was significantly higher on composite nanofibrous scaffolds than PCL nanofibrous scaffolds during 10 days of culture period (Fig. 8). In PCL/HA/Gel composite nanofibrous scaffolds without HA and Gel, mineral deposition was significantly lower up to 66% than in PCL nanofibrous scaffolds. Based on these in vitro results, PCL/HA/Gel composite nanofibrous scaffold developed in this study is considered to recruit favorable adhesion and growth of osteoblasts, as well as to stimulate them for mineralization to exhibit functional activity of osteoblasts for the regeneration of bone.

CONCLUSION

The electrospun PCL/HA/Gel composite nanofibrous scaffold proved to have significantly improved osteoblast responses when compared to those of other nanofibrous scaffolds. The interconnecting porous structure of composite nanofibrous scaffold provided large surface area for cell attachment and proliferation. Osteoblasts cultured on composite nanofibrous scaffold showed higher proliferation rate and a moderate increase in ALP activity and mineralization through the activation of HA and forming multilayer of cells inside and on the surface of the composite nanofibrous scaffolds. The tensile property of composite nanofibrous scaffold was highly flexible and allows penetrating osteoblasts inside the scaffold for proliferation and increased mineralization. Based on these studies, electrospun PCL/HA/Gel composite nanofibrous scaffold is considered as a promising material for bone tissue regeneration.

Acknowledgments: This study was supported by the Office of Life Sciences in the National University of Singapore, and StemLife Sdn Bhd, 50450 Kuala Lumpur, Malaysia.

REFERENCES

1. Vacanti JP, Langer R. Tissue engineering: the design and fabrication of living replacement devices for surgical reconstruction and transplantation. *Lancet* 1999;354:S132–4.
2. Logeart-Avramoglou D, Anagnostou F, Bizios R, Petite H. Engineering bone: challenges and obstacles. *J Cell Mol Med* 2005;9:72–84.
3. Kokubo T, Kim HM, Kawashita M. Novel bioactive materials with different mechanical properties. *Biomaterials* 2003;24: 2161–5.
4. Kim HW, Kim HE, Salih V. Stimulation of osteoblast responses to biomimetic nanocomposites of gelatin–

hydroxyapatite for tissue engineering scaffolds. *Biomaterials* 2005;26:5221–30.
5. Fong H, Chun I, Reneker DH. Beaded nanofibers formed during electrospinning. *Polymer* 1999;40:4585–92.
6. Dzenis Y. Material science. Spinning continuous fibers for nanotechnology. *Science* 2004;304:1917–9.
7. Chapekar MS. Tissue engineering: challenges and opportunities. *J Biomed Mater Res* 2000;53:617–20.
8. Li WJ, Laurencin CT, Caterson EJ, Tuan RS, Ko FK. Electrospun nanofibrous structure: a novel scaffold for tissue engineering. *J Biomed Mater Res* 2002;60:613–21.
9. Venugopal J, Zhang YZ, Ramakrishna S. In vitro culture of human dermal fibroblasts on electrospun polycaprolactone collagen nanofibrous membrane. *Artif Organs* 2006;30:438–44.
10. Zhang YZ, Ouyang HW, Lim CT, Ramakrishna S, Huang ZM. Electrospinning of gelatin fibers and gelatin/PCL composite fibrous scaffolds. *J Biomed Mater Res B* 2005;72:156–65.
11. Badami AS, Kreke MR, Thompson MS, Riffle JS, Goldstein AS. Effect of fiber diameter on spreading, proliferation, and differentiation of osteoblastic cells on electrospun poly(lactic acid) substrates. *Biomaterials* 2006;27:596–606.
12. Ma PX, Langer R. Fabrication of biodegradable polymer foams for cell transplantation and tissue engineering. In: Yarmush M, Morgan J, eds. *Tissue Engineering Methods and Protocols*. Totowa, NJ: Humana Press, 1999;47–56.
13. Bignon A, Chouteau J, Chevalier J, Fantozzi G, Carret J-P, Chavassieux P. Effect of micro- and macroporosity of bone substitutes on their mechanical properties and cellular response. *J Mater Sci Mater Med* 2003;14:1089–97.
14. Hing KA, Best SM, Tanner KE, Bonfield W, Revell PA. Mediation of bone ingrowth in porous hydroxyapatite bone graft substitutes. *J Biomed Mater Res A* 2002;68:187–200.
15. Hing KA, Annaz B, Revell PA, Buckland T. Microporosity enhances bioactivity of synthetic bone graft substitutes. *J Mater Sci Mater Med* 2005;16:467–75.
16. Habibovic P, Yuan H, Van der Valk CM, Meijer G, De Groot K. 3D microenvironment as essential element for osteoinduction by biomaterials. *Biomaterials* 2005;26:3565–75.
17. Woodard JR, Hilldore AJ, Lan SK, Jamison RD, Johnson AJW. The mechanical properties and osteoconductivity of hydroxyapatite bone scaffolds with multi-scale porosity. *Biomaterials* 2007;28:45–54.
18. Chang MC, Ko CC. Preparation of hydroxyapatite–gelatin nanocomposite. *Biomaterials* 2003;24:2853–62.
19. Ito Y, Hasuda H, Kamitakahara M, Ohtsuki C, Tanihara M, Kwon OH. A composite of hydroxyapatite with electrospun biodegradable nanofibers as a tissue engineering material. *J Biosci Bioeng* 2005;100:43–9.
20. Clarke KI, Graves SE, Wong ATC, Triffitt JT, Francis MJO, Czernuszka JT. Investigation into the formation and mechanical properties of a bioactive material based on collagen and calcium phosphate. *J Mater Sci Mater Med* 1993;4:107–10.
21. Wahl DA, Czernuszka JT. Collagen–hydroxyapatite composites for hard tissue repair. *Eur Cell Mater* 2006;11:43–6.
22. Barhate RS, Chong KL, Ramakrishna S. Preparation and characterization of nanofibrous filtering media. *J Memb Sci* 2006;283:209–18.
23. Jena A, Gupta K. Pore volume of nanofiber nonwovens. *Int Nonovens J* 2005;25–30.
24. Gregory CA, Gunn WG, Peister A, Prockop DJ. An Alizarin red-based assay of mineralization by adherent cells in culture: comparison with cetylpyridinium chloride extraction. *Anal Biochem* 2004;329:77–84.
25. Causa F, Netti PA, Ambrosio L, et al. Poly-epsilon-caprolactone/hydroxyapatite composites for bone regeneration: in vitro characterization and human osteoblast response. *J Biomed Mater Res A* 2006;76:151–62.
26. Teixeira AI, Nealey PF, Murphy CJ. Responses of human keratocytes to micro and nanostructured substrates. *J Biomed Mater Res A* 2004;71:369–76.
27. Hamlin NJ, Price PA. Mineralization of decalcified bone occurs under cell culture conditions and requires bovine serum but not cells. *Calcif Tissue Int* 2004;75:231–42.
28. Zhang YZ, Feng Y, Huang ZM, Ramakrishna S, Lim CT. Fabrication of porous electrospun nanofibres. *Nanotechnology* 2006;17:901–8.
29. Webster TJ, Ergun C, Doremus RH, Siegel RW, Bizios R. Specific proteins mediate enhanced osteoblast adhesion on nanophase ceramics. *J Biomed Mater Res A* 2000;51:475–83.
30. Webster TJ, Siegel RW, Bizios R. Osteoblast adhesion on nanophase ceramics. *Biomaterials* 1999;20:1221–7.
31. Anselme K. Osteoblast adhesion on biomaterials. *Biomaterials* 2000;21:667–81.
32. Grinnell F. Focal adhesion sites and the removal of substratum-bound fibronectin. *J Cell Biol* 1986;103:2697–706.
33. Li M, Mondrinos MJ, Chen X, Gandhi MR, Ko FK, Lelkes PI. Co-electrospun poly(lactide-co-glycolide), gelatin, and elastin blends for tissue engineering scaffolds. *J Biomed Mater Res A* 2006;79:963–73.
34. Malaval L, Liu F, Roche P, Aubin JE. Kinetics of osteoprogenitor proliferation and osteoblast differentiation in vitro. *J Cell Biochem* 1999;74:616–27.
35. Ogata K, Imazato S, Ehara A, Nakano T, Umakoshi Y. Comparison of osteoblast responses to hydroxyapatite and hydroxyapatite/soluble calcium phosphate composites. *J Biomed Mater Res A* 2005;72:127–35.